minerals

MDPI

Article

Study on the Reverse Flotation Separation of Smithsonite from Dolomite Using the Saponified 2-(4,4-Dimethylpentan-2-yl)-5,7,7-trimethyloctanoic Acid as a Collector

Xiaoliang Zhang [1], Yangge Zhu [1,*], Zhiqiang Zhao [1] and Peilong Wang [2]

[1] BGRIMM Technology Group, State Key Laboratory of Mineral Processing, Beijing 102600, China; heutzxl2009@126.com (X.Z.); zhaozhiqiang@bgrimm.com (Z.Z.)
[2] Civil and Resources Engineering School, University of Science and Technology Beijing, Beijing 100083, China; wangpeilong@ustb.edu.cn
* Correspondence: zhuyangge@126.com

Abstract: Dolomite, a prominent calcium-bearing gangue mineral found in carbonate-type zinc oxide ores, poses a significant challenge for effective flotation separation alongside smithsonite due to their highly similar surface properties. The present study explores the potential of 2-(4,4-dimethylpentan-2-yl)-5,7,7-trimethyloctanoic acid (2-DMPT) as a collector for the reverse flotation of smithsonite from dolomite. Micro-flotation experiments indicated that saponified 2-DMPT exhibited superior collecting ability and selectivity for dolomite over smithsonite under highly alkaline conditions. Specifically, the flotation recovery of dolomite reached 62%, whereas only 6% of smithsonite was recovered in the flotation foam products. Zeta potential and attenuated total reflectance–Fourier transform infrared (ATR-FTIR) analysis revealed that changes in pH values had minimal influence on the collector's adsorption onto dolomite, while significantly hindering its adsorption on the smithsonite surface. Furthermore, X-ray photoelectron spectroscopy (XPS) analysis showed that 2-DMPT could form hydrophobic complexes with the active Ca^{2+} sites on the dolomite surface at pH 11.5. However, the interaction between smithsonite and carboxylic groups of 2-DMPT under the same conditions was relatively weaker, facilitating their reverse flotation separation. As a result, 2-DMPT shows promise as a potential collector for the reverse flotation process, effectively removing dolomite from smithsonite and reducing acid consumption in subsequent acid-leaching processes.

Keywords: smithsonite; dolomite; reverse flotation; highly alkaline conditions; saponified 2-DMPT

Citation: Zhang, X.; Zhu, Y.; Zhao, Z.; Wang, P. Study on the Reverse Flotation Separation of Smithsonite from Dolomite Using the Saponified 2-(4,4-Dimethylpentan-2-yl)-5,7,7-trimethyloctanoic Acid as a Collector. *Minerals* **2023**, *13*, 1322. https://doi.org/10.3390/min13101322

Academic Editor: Hyunjung Kim

Received: 11 August 2023
Revised: 8 September 2023
Accepted: 12 September 2023
Published: 13 October 2023

1. Introduction

In 2022, global mine production of zinc was approximately 13 million tonnes, and demand for zinc resources will increase with the growth of the global economy [1]. Zinc oxide ore accounts for 23% of the world's known zinc ore reserves, and China has low-grade zinc oxide ores of over 30 million tons, which are stockpiled on site and cannot be further processed [2]. Therefore, the efficient utilization of such zinc ore resources has become increasingly important and is seen as an inevitable path to meet the zinc demand of the industry. Smithsonite, an important zinc oxide mineral with industrial value, is commonly associated with carbonate minerals such as dolomite and calcite [3]. Froth flotation is the common method to concentrate smithsonite from zinc oxide ores, and it can be divided into direct flotation and sulfidization flotation. Direct flotation using fatty acids or their derivatives as flotation collectors is an effective method for smithsonite beneficiation. These polar collectors absorb onto smithsonite particles, resulting in the hydrophobization of the particles and improving their floatability [4,5]. Wang et al. used a mixed collector of sodium oleate (NaOL) and benzohydroxamic acid (BHA) to separate smithsonite from dolomite by direct flotation. The flotation recovery of smithsonite reached 92%, while it was less than 20% for dolomite when the molar ratio of NaOL/BHA was set to 2:1 [6]. Luo

et al. found that 2-(hexadecanoylamino) acetic acid, a 16-carbon saturated fatty acid that is amide-linked to glycine, is an effective collector for the flotation of smithsonite. The recovery of smithsonite exceeded 90% at a collector concentration of 2×10^{-4} mol·L^{-1} and pulp pH of 9.0, while the recovery of dolomite did not reach 10% [7].

However, fatty acids are also commonly used as collectors to float calcium-bearing carbonate minerals directly from the ore [8]. This can be a challenge when a large number of magnesite and calcium carbonate gangues are present, as the floatability of these minerals is similar to that of smithsonite. To solve this problem, some researchers have attempted to develop selective inhibitors to increase the difference in the floatability of smithsonite and dolomite/calcite. Several polymer anionic surfactants, including fenugreek gum [9], flaxseed gum [10], guar gum [11], and calcium lignosulphonate [12], have been shown to be effective inhibitors for the selective flotation separation of smithsonite and calcite. Moreover, some organic acids, e.g., polyepoxysuccinic acid [13], phenylpropenyl hydroxamic acid [14], phytic acid [15], 2-phosphonobutane-1,2,4-tricarboxylic acid [16], have also been found to have excellent selective inhibitory effects on calcite, while having a negligible effect on smithsonite when using sodium oleate as the flotation collector. Wang et al. demonstrated that sodium hexametaphosphate is chemically adsorbed on the dolomite surface in the form of hydrophilic complexes with active Ca^{2+} and Mg^{2+} sites, which significantly inhibits the subsequent adsorption of the mixed benzohydroxamic acid and sodium oleate collector [17]. Although several selective depressants for the separation of smithsonite and dolomite/calcite have been reported in recent studies, these reagents have not been able to overcome the challenges of high dosage, high cost, chemical toxicity, or, to some extent, depressing smithsonite flotation [15,18]. Therefore, the efficient flotation separation of smithsonite and calcium-bearing carbonate minerals (e.g., dolomite and calcite) using direct flotation remains a challenging task.

Sulfidization-amine flotation is widely employed for beneficiating low-grade zinc oxide ores in industrial operations. However, this process is encumbered by challenges, including difficulties in controlling the sulfidization process, high reagent consumption, suboptimal selectivity, and inadequate recovery efficiency for zinc oxide minerals [19,20]. Prior desliming is indispensable to achieve effective smithsonite recovery using the sulfidization-amine method due to the considerable sensitivity and poor selectivity of amine-type collectors towards slime [21,22]. Nevertheless, a major drawback of this approach is the substantial loss of Zn metal during the pretreatment stage. Additionally, eliminating flotation foam becomes arduous, and enormous reagent consumption is necessary when employing amines as collectors in the sulfurized flotation process, particularly for ores containing highly weathered sludges [23]. Consequently, the application of sulfidization-amine flotation is currently limited to high-grade zinc oxide ores within the industry.

It is well known that smithsonite is difficult to float due to its poor floatability, but it can be easily dissolved in an acidic solution. Acid leaching is considered to be a more efficient method for zinc extraction from smithsonite, especially for low-grade zinc oxide ores. However, the presence of carbonate gangue minerals can increase acid consumption during leaching, limiting the widespread application of acid leaching in industrial practice for the treatment of carbonate-rich zinc oxide ores [24]. The literature reports that carbonate gangue minerals, such as calcite and dolomite, are more easily floated by fatty acid collectors than smithsonite [25]. A few studies have reported that fatty acids can be used as collector reagents to remove most unwanted carbonate, sulfate, silicate, and ferrous gangue minerals in zinc rough concentrates by reverse flotation, further increasing the concentrate zinc grade [26]. Zhang discovered that sodium oleate mixed with the bridging liquid, such as kerosene or benzene, could be used as a high-selectivity collector to separate calcite from zinc oxide ores via reverse flotation. Over 90% calcite was recovered in the flotation foam products with the collector NaOL dosage of 4000 g/t, and the acid consumption was reduced by 65% after calcium reverse flotation [27]. In addition, reverse flotation using Na-Oleate in combination with the non-ionic additive (NI2) has also been applied to the treatment of complex carbonate-rich copper-cobalt mixed ores at acidic pH (4.5–5). The

products obtained in the flotation tank by this process were further processed by acid leaching, increasing the overall copper and cobalt recoveries [28]. Therefore, considering the perspective of beneficiation and metallurgy cooperation, the pre-removal of carbonate gangue minerals in low-grade zinc oxide ores via reverse flotation followed by hydrometallurgical methods is necessary and feasible. This is expected to significantly increase the overall recovery of zinc from low-grade zinc oxide ores.

In this study, the flotation collector 2-(4,4-dimethylpentan-2-yl)-5,7,7-trimethyloctanoic acid (2-DMPT) was evaluated for its ability to separate dolomite from smithsonite via reverse flotation. 2-DMPT is a saturated branched-chain fatty acid that can be synthesized from a variety of starting materials including fatty acids, esters, and alcohols. It has a valuable combination of saturation and branching, which makes it more effective than straight-chain fatty acids for the flotation of calcium-bearing minerals. Zhang et al. investigated the effect of fatty acid structure on the flotation behavior of scheelite, a calcium-bearing salt-type mineral. They found that branched-chain fatty acids had better collecting capacity for scheelite flotation than straight-chain fatty acids [29]. This study builds on this previous work by investigating the use of 2-DMPT for the flotation of dolomite, a major calcium-bearing carbonate gangue mineral of smithsonite. Micro-flotation experiments were conducted to investigate the flotation performance of the two minerals. Zeta potential measurement, ATR-FTIR, and XPS analysis were also conducted to understand the adsorption mechanism of 2-DMPT on the mineral surfaces. This study could have significant implications for the extraction of zinc from carbonate-rich zinc oxide ores, as it could help to reduce acid consumption in the subsequent acid-leaching process and increase the overall recovery of zinc.

2. Materials and Methods

2.1. Minerals and Reagents

High-purity dolomite ($CaMg[CO_3]_2$) and smithsonite ($ZnCO_3$) samples were purchased from Huadong Ye's Stone Specimen Firm, Guangdong Province, China. The mineral samples were first crushed to less than 5 mm using a hammer, and then ground in a ceramic ball mill separately. The ground samples were wet-sieved to a size fraction of $-74 + 38$ μm, which were used for X-ray diffraction (XRD) measurements, micro-flotation tests, XPS, and ATR-FTIR analysis. The samples with particle sizes less than 38 μm were used for zeta potential measurements. The high purity of the prepared dolomite and smithsonite samples was confirmed by multi-element chemical analysis, with purities above 97% and 95%, respectively. Table 1 summarizes the results of the chemical analysis. X-ray diffraction (XRD) was used to further investigate the crystal structures of the mineral phases. The XRD patterns were collected using a Rigaku D/MAX-2600 with Cu Kα radiation (λ = 1.5406 Å) at a scanning speed of $2^\circ \cdot min^{-1}$. The experimental XRD patterns were well-matched with the standard pattern of dolomite (JCPDS 36-0426) and smithsonite (JCPDS 08-0449), and no obvious impurity peaks were observed. The XRD analysis results confirmed that both dolomite and smithsonite samples were of high purity and could meet the experimental requirements. Rietveld refinement was performed on the experimental XRD patterns to obtain the structural information of the mineral phases. The Rietveld refinement profiles of XRD data for pure dolomite and smithsonite samples are shown in Figure 1. The good agreement between the experimental data (red dots line) and calculated values (solid black line) suggests that the results of crystal-structure refinement are accurate and reliable. The chi-square (Chi^2) values for Rietveld refinement profiles of XRD patterns of dolomite and smithsonite are 2.42 and 2.91, respectively. The other detailed variation of R-factors in Rietveld analysis and the lattice parameters of dolomite and smithsonite are presented in Table 2. The XRD patterns of the two carbonate minerals have both been indexed by a rhombohedral (hexagonal setting) lattice system with the trigonal R3c space group. The crystal structures of dolomite and smithsonite are extremely similar, with only minor differences in the atomic positions. This explains the difficulty in separating the two minerals by flotation.

Table 1. Chemical compositions of the dolomite and smithsonite mineral samples (wt.%).

Sample	$CaCO_3$	$MgCO_3$	SiO_2	Al_2O_3	TFe	$ZnCO_3$	Others
Dolomite	53.73	44.63	0.41	0.04	0.05	/	1.14
Smithsonite	/	/	0.11	0.01	0.42	95.52	3.94

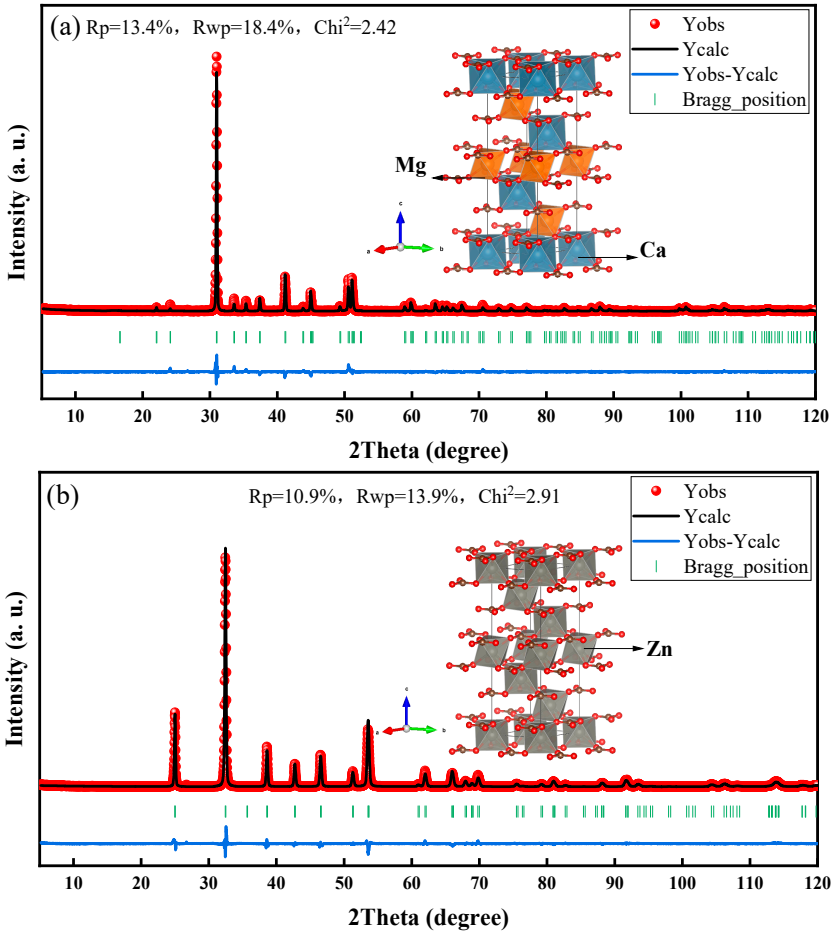

Figure 1. Rietveld refinement profile of XRD patterns of the prepared dolomite (**a**) and smithsonite (**b**) samples at room temperature, measured at a scanning speed of $2^{\circ}\cdot min^{-1}$.

Table 2. Refined lattice parameters and the R-factors in Rietveld analysis for dolomite and smithsonite.

Sample	Space Group	Lattice Parameters (Å)		Volume ($Å^3$)	*R*-Factors		
		$a = b$	c		R_{wp} (%)	R_{wp} (%)	Chi^2
Dolomite	R3c	4.8072	16.0099	320.413	13.4	18.4	2.42
Smithsonite	R3c	4.6643	15.1037	284.574	10.9	13.9	2.91

In this study, a saturated branched-chain fatty acid 2-DMPT was introduced as a collector to realize the separation of smithsonite and dolomite through reverse flotation. The flotation collector 2-DMPT underwent saponification treatment with sodium hydroxide in a 1:1 mole ratio. The molecular structure of 2-DMPT, which was procured from Shanghai Aladdin Biochemical Technology Co., Ltd. (China), is illustrated in Figure 2. Analytical reagent grade sodium hydroxide (NaOH) and hydrochloric acid (HCl) for pH adjustment were obtained from Sinopharm Chemical Reagent Co. Ltd., and deionized water was used in all micro-flotation tests and other measurements.

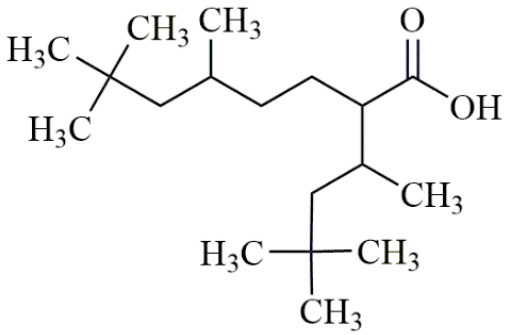

Figure 2. The molecular structure of 2-DMPT.

2.2. Micro-Flotation Tests

Micro-flotation tests were conducted using an XFG flotation machine equipped with a 40 mL plexiglass cell (Jilin Exploration Machinery Plant, Changchun, China). Each run involved a 2.0 g mineral sample was mixed with 35 mL deionized water in the flotation cell. The spindle speed of the flotation machine was set to 1500 rpm. The mass ratio of dolomite to smithsonite was 1:1 in the artificially mixed minerals micro-flotation tests. Before adding flotation reagents, the pulp was stirred for 3 min to ensure full mineral particle dispersion. Subsequently, the pulp was adjusted to the desired pH using NaOH or HCl solutions and stabilized for 2 min. The saponified 2-DMPT was then added to the mineral suspension and agitated for an additional 3 min. After that, the flotation froth was manually collected by scraping, and it lasted for 4 min. The flotation foam products and tailings were collected separately, then filtered, dried, and weighed to calculate mineral recovery according to the following Equation (1). For the flotation separation of artificially mixed minerals, the same experimental procedures were conducted as described above, and the flotation recovery was calculated by Equation (2) after assaying the foam products and flotation tailings. Each flotation test was conducted in triplicate, and the average results were calculated and plotted [30].

$$\varepsilon_{pm} = \frac{m_c}{m_c + m_t} \times 100\% \quad (1)$$

$$\varepsilon_{Zn/\mathrm{Ca}} = \frac{m_c \times \beta_1}{m_c \times \beta_1 + m_t \times \beta_2} \times 100\% \quad (2)$$

where ε_{pm} refers to the flotation recovery of pure dolomite or smithsonite minerals and m_c (g) and m_t (g) are the weight of concentrates and tailings, respectively. The $\varepsilon_{Zn/\mathrm{Ca}}$ denotes the flotation recovery of smithsonite or dolomite in flotation foam products, and β_1 and β_2 stand for the grade of Zn or Ca in the flotation foam products and tailings, resepctively.

2.3. Zeta Potential Measurement

Zeta potential measurements for the dolomite and smithsonite samples were conducted using the NS-90 nanometer particle size analyzer (Zhuhai OMEC Instruments Co., Ltd., Zhuhai, China). Prior to performing the zeta potential tests, mineral samples with particle sizes less than 38 μm were further ground using an agate mortar. Particle-size distribution analysis confirmed that the D(50) values for smithsonite and dolomite samples were 12.46 μm and 7.72 μm, respectively. For each test, 20 mg of pure mineral samples were dispersed in 35 mL of KCl background electrolyte (1.0×10^{-3} mol·L^{-1}). The mineral suspension was continuously stirred on a magnetic stirrer and adjusted to the desired pH value using HCl or NaOH solutions, and a collector was added if required. After 10 min of magnetic stirring, 2 mL of supernatant liquor was extracted for zeta potential measurement. Each independent test was repeated three times under specific reagent conditions to obtain the average value and error bars of the zeta potential.

2.4. ATR-FTIR Spectroscopy

Fourier-transform infrared spectroscopy (FTIR) is a well-established analytical technique used to obtain chemical and structural information of samples by identifying characteristic vibrational frequencies of functional groups in the infrared (IR) region [31]. In this work, ATR-FTIR spectroscopy was employed to investigate the surface chemical functional groups of powdered mineral particles. The ATR mode allows for efficient and accurate analysis of the samples. The ATR-FTIR analysis was performed on powdered mineral samples with the Thermo Scientific Nicolet iS20 FTIR Spectrometer equipped with a deuterated triglycine-sulphate (DTGS) detector and a variable-angle ATR accessory. The particle size of the smithsonite and dolomite samples used was between 38 μm to 74 μm, which matched that of the micro-flotation tests. The samples were mixed with the collector at pH 11.5 in a 40 mL flotation cell. After a conditioning period of 10 min at 1500 rpm, the slurry was filtered, flushed, and naturally dried at room temperature. The ATR-FTIR spectra were recorded with a resolution of 4 cm^{-1} and scanned 32 times to ensure accurate and reliable results. This analysis allowed us to identify and characterize the specific functional groups present on the surface of the mineral particles.

2.5. Depth-Profiling XPS Analysis

X-ray photoelectron spectroscopy was employed to investigate the elemental chemical composition and chemical state transformations on mineral surfaces before and after treatment with the collector saponified 2-DMPT. The XPS analysis was conducted on an ESCALAB 250Xi instrument (Thermo Fisher Scientific, Loughborough, UK) equipped with an Al Ka X-ray source operating at 1486.6 eV and 150 W. High-resolution scanning was performed with a pass energy of 50 eV and a step size of 0.1 eV. Charge correction was achieved using the standard C–C binding energy of 284.8 eV as a reference. The particle size of the samples used for XPS analysis matched that of the micro-flotation tests (38–74 μm). For each test, 1.0 g of mineral samples was dispersed and stirred for 10 min in 40 mL of deionized water, both in the absence and presence of the collector at pH 11.5. Subsequently, the mineral suspensions were filtered, washed with deionized water, and the solid fractions were collected and naturally dried at room temperature in preparation for XPS detection. Finally, the dried samples underwent XPS analysis, and the obtained results were processed and analyzed using the Avantage software to gain insights into the chemical changes occurring on the mineral surfaces due to the interaction with the collector saponified 2-DMPT.

3. Results and Discussion

3.1. Micro-Flotation Results

3.1.1. Micro-Flotation Tests on Single Minerals

The impact of saponified 2-DMPT dosage on the flotation behaviors of smithsonite and dolomite was examined under pH = 9.0 conditions, and the results are depicted in Figure 3. It was observed that the flotation recovery of both minerals increased gradually with the rising concentration of the collector. For dolomite, the flotation recovery reached its peak at a collector dosage of 0.5×10^{-4} mol·L^{-1}, while for smithsonite, the optimum dosage was 1.5×10^{-4} mol·L^{-1}. Notably, the recovery of dolomite consistently surpassed that of smithsonite across the entire concentration range studied, indicating that dolomite was more inclined to be floated to the foam products compared to smithsonite. The difference in flotation recovery between smithsonite and dolomite remained at approximately 30%, even when the concentration of saponified 2-DMPT was increased to 2.5×10^{-4} mol·L^{-1}. Despite some disparity in the floatability of dolomite and smithsonite, this variation was insufficient to enable effective separation of the two carbonate minerals through reverse flotation under the current pulp pH of 9.0.

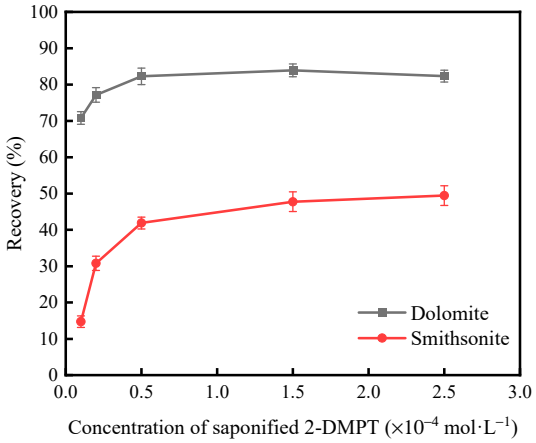

Figure 3. The effect of saponified 2-DMPT dosage on the flotation recoveries of dolomite and smithsonite at the pulp pH of 9.0.

The influence of pulp pH levels on the flotation performance of minerals is well established. Figure 4 illustrates the impact of pH on the flotation behaviors of dolomite and smithsonite, with a constant concentration of the collector fixed at 2.5×10^{-4} mol·L^{-1}. The results reveal distinct differences in their floatability under varying pH conditions. Dolomite exhibited remarkable floatability in highly alkaline conditions, with a consistent recovery of over 80% across the pH range from 9 to 12. As depicted in Figure 4, the floatability of smithsonite exhibited a relatively favorable response within a narrow pH range of 8 to 10, with the recovery of smithsonite declining from 49% to 4% as the pH value increased from 9 to 11.5. Particularly noteworthy is the significant reduction in flotation recovery of smithsonite when subjected to highly alkaline conditions (pH > 11), while the recovery of dolomite remained consistently high. This observation suggests the possibility of effectively separating dolomite from smithsonite in the flotation system using saponified 2-DMPT as the collector under strong alkaline conditions (pH > 11).

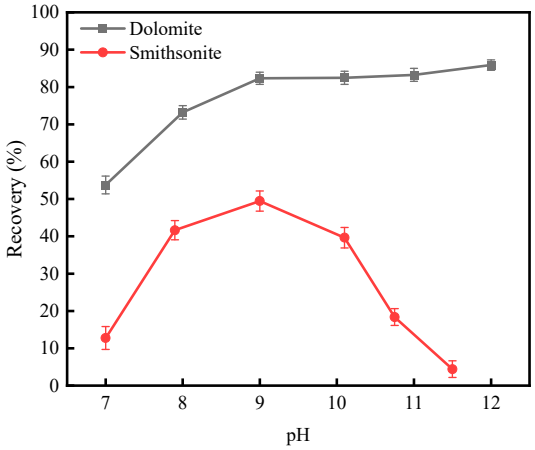

Figure 4. The relation between pH and dolomite and smithsonite recoveries with the concentration of saponified 2-DMPT fixed at 2.5×10^{-4} mol·L^{-1}.

3.1.2. Micro-Flotation Tests on Artificially Mixed Minerals

To further validate the earlier conjecture based on the results of single mineral micro-flotation tests, micro-flotation tests were conducted on artificially mixed minerals of dolomite and smithsonite. The objective was to investigate the impact of saponified 2-DMPT dosage and pulp pH on the separation efficiency of the mixed minerals, maintaining a fixed mass ratio of dolomite to smithsonite (1:1). Figure 5 illustrates the substantial enhancement in the separation efficiency of dolomite and smithsonite under highly alkaline

conditions (pH > 11). Notably, as the pulp pH reached 11.5, only 6% of smithsonite was found in the flotation foam products, while achieving a significant total calcium recovery of 62%. In essence, this implies that more than half of dolomite could be effectively removed through reverse flotation with a collector concentration of 2.5×10^{-4} mol·L^{-1} and a pulp pH of 11.5. Moving on to Figure 6, the influence of saponified 2-DMPT dosage on the flotation separation of the artificially mixed minerals was examined. It was observed that the removal efficiency of calcium steadily increased with higher collector concentrations. However, the flotation recovery of zinc in the flotation concentrates consistently remained below 10%. These observations indicate that elevating the alkalinity of the flotation slurry significantly suppressed the flotation of smithsonite in the presence of saponified 2-DMPT as a collector, especially at a pulp pH of 11.5. In conclusion, the findings demonstrate that 2-DMPT can effectively serve as a collector for selectively removing a portion of dolomite from carbonate-type zinc oxide ores, consequently reducing acid consumption during subsequent acid-leaching processes.

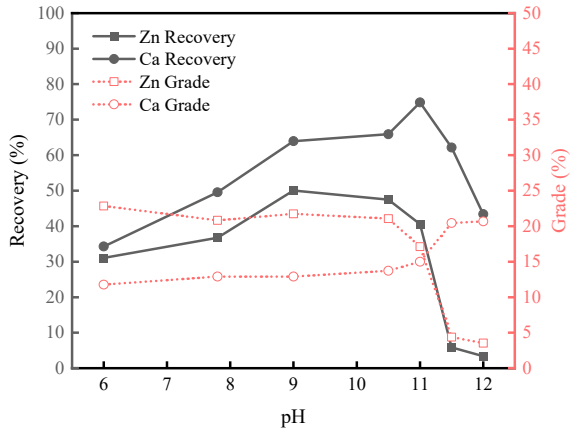

Figure 5. The effect of pulp pH on the flotation separation results of artificially mixed minerals with a fixed collector concentration of 2.5×10^{-4} mol·L^{-1}.

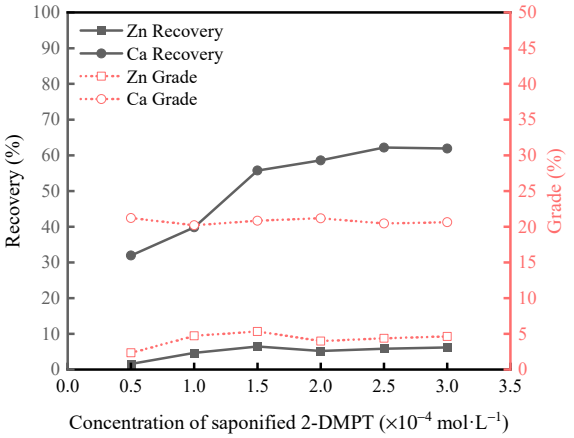

Figure 6. The effect of saponified 2-DMPT dosage on the flotation separation results of artificially mixed minerals at pH 11.5.

3.2. Zeta Potential Measurement Results

Zeta potential plays a crucial role in the flotation of oxide and silicate minerals as it governs the absorption of flotation reagents at the mineral–water interface [32]. Micro-flotation test results have demonstrated the excellent potential of 2-DMPT for removing dolomite from carbonate-type zinc oxide ores by reverse flotation under highly alkaline conditions (pH = 11.5). Understanding the changes in the charge on mineral surfaces is vital in comprehending the interaction between minerals and collectors in the flotation

system. Consequently, the dynamic potential changes of dolomite and smithsonite before and after treatment with the saponified 2-DMPT at pH 11.5 were investigated through zeta-potential measurements, and the relevant results are presented in Figures 7 and 8. Figure 7 reveals the isoelectric points (IEP) of pure dolomite and smithsonite at around pH 6.0 and 8.9, respectively, in agreement with previous research [33–35]. As the pulp pH increased, the zeta potential of both dolomite and smithsonite decreased due to the absorption of hydroxide ions (OH^-) in alkaline solutions. Moreover, smithsonite exhibited a higher surface charge than dolomite under alkaline conditions. For instance, at pH 11, the zeta potential of smithsonite measured approximately −29.97 mV, whereas that of dolomite was determined to be −10.67 mV. This observation indicates a notably stronger interaction between hydroxide ions (OH^-) and the smithsonite surface compared to dolomite.

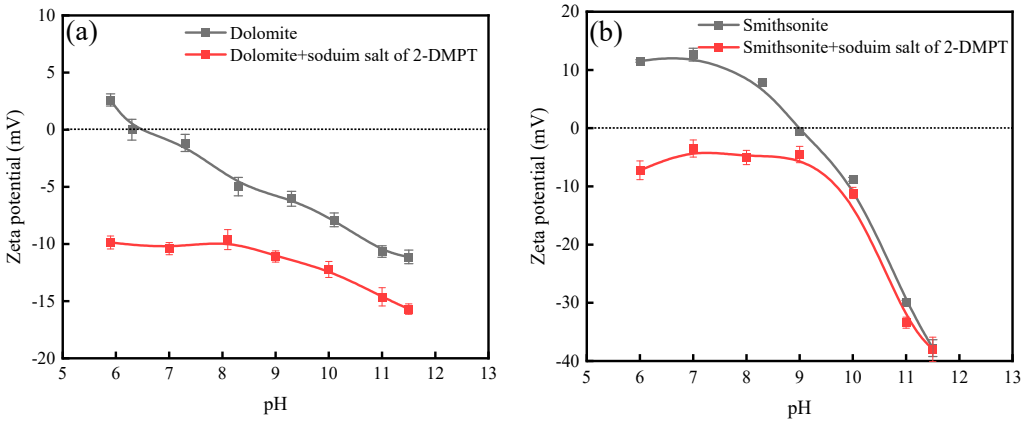

Figure 7. Zeta potential of dolomite (**a**) and smithsonite (**b**) after conditioning with deionized water and the sodium salt of 2-DMPT as a function of pH values.

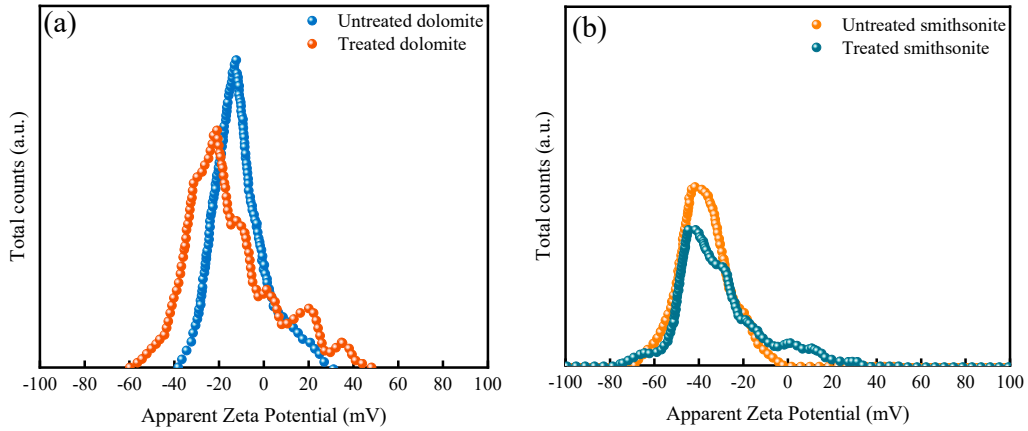

Figure 8. Zeta potential distribution of dolomite (**a**) and smithsonite (**b**) untreated and treated with the sodium salt of 2-DMPT at pH 11.5.

Upon addition of the anionic collector 2-DMPT, both dolomite and smithsonite exhibited negative shifts in zeta potentials across the entire studied pH range, indicating the adsorption of the sodium salt of 2-DMPT on their surfaces. However, noteworthy differences emerged as pH values exceeded 11, with smithsonite's zeta potential changes becoming much smaller, stabilizing below 3.50 mV. This suggests a strong inhibition of the interaction between smithsonite and the collector 2-DMPT under alkaline conditions. Additionally, Figure 8 illustrates the zeta potential distribution of smithsonite remained nearly unchanged before and after treatment with the sodium salt of 2-DMPT at pH 11.5, with the zeta potential value fluctuated around 38 mV. In contrast, dolomite experienced a significant decline from −11.13 mV to −15.70 mV under the same conditions. This decline can be attributed to the absorption of negatively charged 2-DMPT anions onto the dolomite

surface. Therefore, it is concluded that an increase in the slurry pH selectively inhibited the subsequent absorption of saponified 2-DMPT on the surface of smithsonite.

3.3. ATR-FTIR Spectra Analysis

In this study, 2-DMPT was utilized as a collector after undergoing saponification treatment with sodium hydroxide. As seen in Figure 9, characteristic peaks at 2952.13 cm^{-1} and 2867.59 cm^{-1} corresponded to the stretching vibrations of the $(–CH_2–)_n$ group in the branched-chain 2-DMPT [15,36]. The symmetric deformation vibration of the methylene group was detected at 1466.96 cm^{-1}. Additionally, a prominent peak located at 1701.59 cm^{-1} was attributed to the stretching vibration of C=O, while the symmetric vibration peak of the carboxyl group (–COO–) appeared at 1393.43 cm^{-1} [37,38]. The ATR-FTIR spectra of untreated dolomite and smithsonite, as well as their treated counterparts with saponified 2-DMPT at pH 11.5, were compared and analyzed. Figure 10 shows the ATR-FTIR difference spectra of the two minerals after interaction with the collector at pulp pH 11.5. For dolomite, significant variations occurred in the range of 3050–2800 cm^{-1} after treatment, where three new characteristic absorption peaks emerged, stemming from the stretching vibration peak of C–H in the branched-chain 2-DMPT. However, in comparison to the original spectrum of pure smithsonite, no significant changes were observed in the range of 3050–2800 cm^{-1} after treatment with saponified 2-DMPT at pH 11.5. Notably, a distinct broad peak around 1050–1710 cm^{-1} was observed, providing further evidence that the carboxyl group of 2-DMPT was absorbed onto mineral surfaces. These findings imply the formation of stable chemisorption of saponified 2-DMPT on the dolomite surface, whereas it exhibited weaker absorption on the smithsonite surface at pH 11.5. Considering the results from the zeta potential analysis, it is evident that saponified 2-DMPT is likely to be adsorbed on the surface of dolomite rather than smithsonite under highly alkaline conditions.

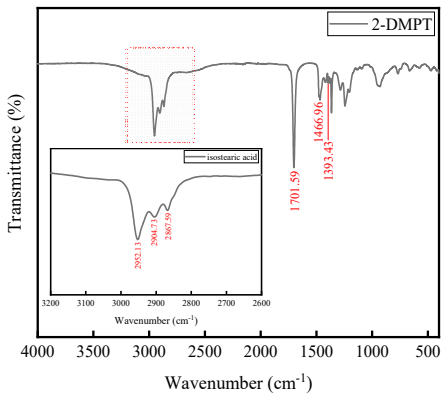

Figure 9. ATR-FTIR spectrum of 2-(4,4-Dimethylpentan-2-yl)-5,7,7-trimethyloctanoic acid 2-DMPT.

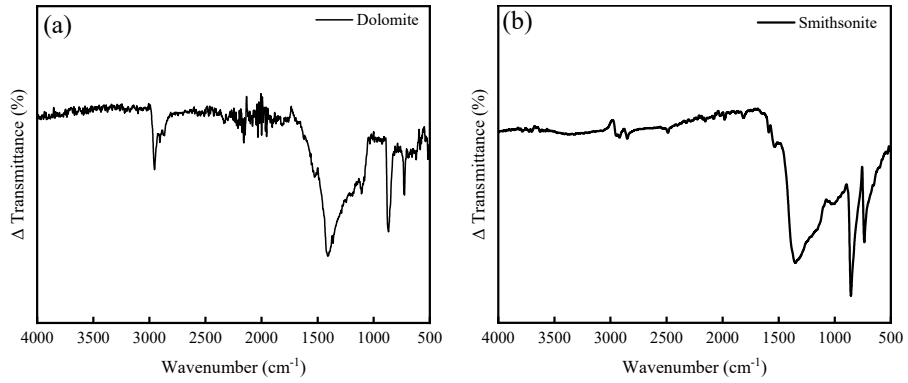

Figure 10. FTIR difference spectroscopy by ATR to characterize the absorption state of saponified 2-DMPT on of dolomite (**a**) and smithsonite (**b**) surfaces at pH 11.5.

3.4. XPS Depth Profile Analysis

To gain further insights into the mechanism of reverse flotation separation of dolomite from smithsonite under highly alkaline conditions with saponified 2-DMPT, XPS depth profiling was conducted on the dolomite and smithsonite samples after treatment with the collector at pH 11.5. This analysis aimed to determine the element compositions and chemical states on mineral surfaces and near-surfaces. Figure 11 shows the changes in elemental concentrations on the treated dolomite and smithsonite surfaces as a function of etching time. It is evident that the atomic carbon concentration on mineral surfaces and near-surfaces experienced a sharp decrease within the initial 25 s of etching (0.2 nm/s). In contrast, the concentration of metal elements, such as calcium, magnesium, and zinc, exhibited a gradual increase with extended etching time. This observation indicates that the adsorption layer's thickness on the mineral surface should be within 5 nm.

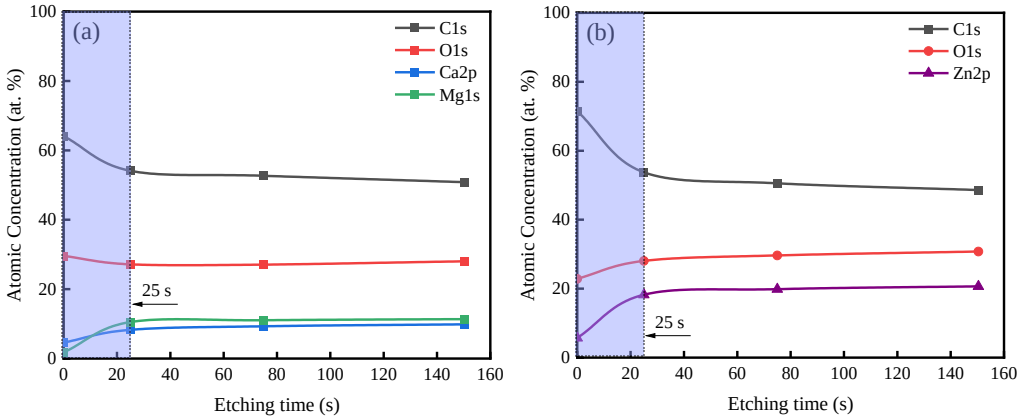

Figure 11. XPS depth profile of the constituent elements as measured on the dolomite (**a**) and smithsonite (**b**) samples after conditioning with the sodium salt of 2-DMPT at pH 11.5.

In addition, X-ray photoelectron spectroscopy (XPS) enables the determination of chemical shifts in electron binding energies of specific elements, offering insights into the changes in the chemical environment surrounding the atoms involved [39]. High-resolution XPS spectra of the treated dolomite sample were collected at different etching times of 0, 25, and 150 s, and the fitted results are displayed in Figure 12. Figure 12a illustrates the C 1s spectrum of the bare dolomite surface (etching time = 0 s) treated with saponified 2-DMPT at pH 11.5, which was fitted into four different carbon species. The C 1s peak at 289.15 eV was attributed to the absorption of the carboxylic group (–COOR) [40,41]. Notably, the C 1s peak located at a binding energy of 289.15 eV disappeared, while the signal of carbonate ion (CO_3^{2-}) around 290.50 eV intensified at etching times of 25 s and 150 s. Additionally, the primary signal of C–C bond located at 284.80 eV gradually decreased with the increasing sputtering depth. Figure 12b displays the high-resolution Ca 2p spectra of the bare dolomite surface, deconvoluted into two spin-orbit doublet peaks of Ca $2p_{1/2}$ and Ca $2p_{3/2}$. The Ca $2p_{3/2}$ peak centered at 347.02 eV and 347.56 eV originated from the carbonate ion (CO_3^{2-}) and Ca^{2+}–COO– ionic complexation, respectively [42,43]. In Figure 13c, two peaks centered at 533.40 eV and 531.65 eV were observed before sputtering, corresponding to oxygen atoms in the carboxylic group and metal carbonates, respectively [44,45]. After a 25-s sputtering treatment, the O 1s peak corresponding to carboxylic groups disappeared, suggesting complete removal of the absorption layer on the surface of dolomite. Meanwhile, a new low-energy peak at 529.45 eV emerged in the O 1s spectra, assigned to the O atoms in the bulk phase bound to metals (e.g., Ca, Mg and Zn) [46,47]. Additionally, the signal strength of bulk lattice oxygen gradually increased with the increasing sputtering depth. These findings provide valuable insights into the chemical changes occurring on the dolomite surface during the interaction with saponified 2-DMPT under highly alkaline conditions.

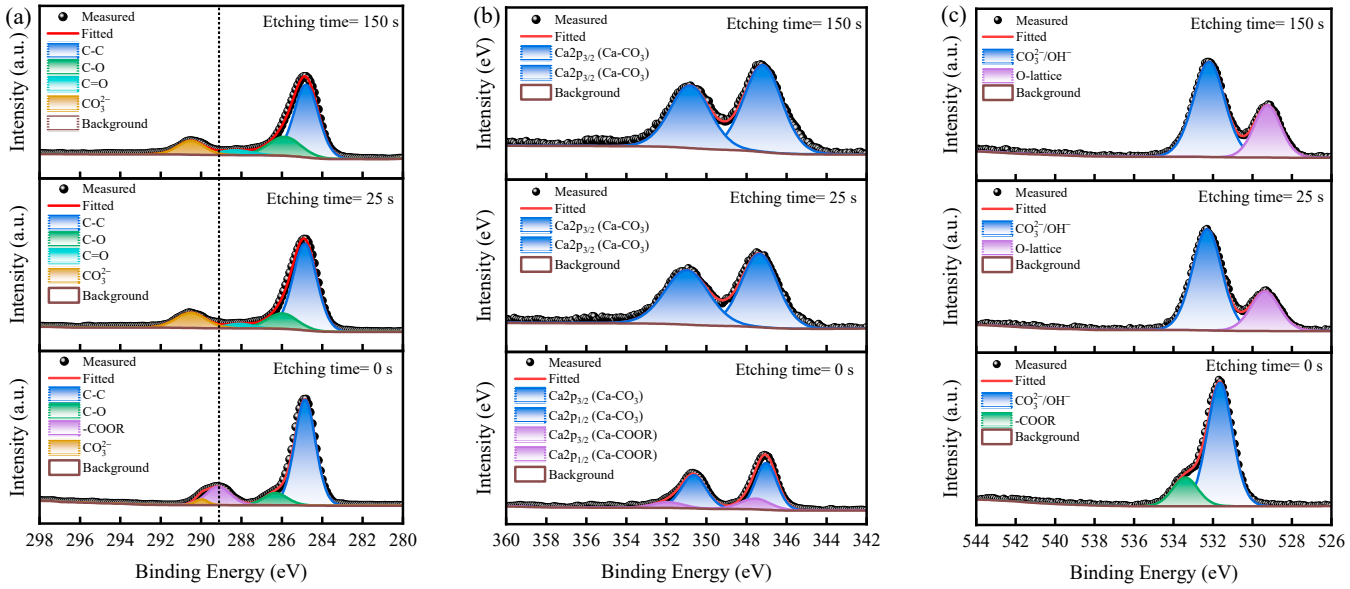

Figure 12. Depth profiling high-resolution XPS C 1s (**a**), Ca 2p (**b**) and O 1s (**c**) spectra of the dolomite sample after conditioning with the sodium salt of 2-DMPT at pH 11.5.

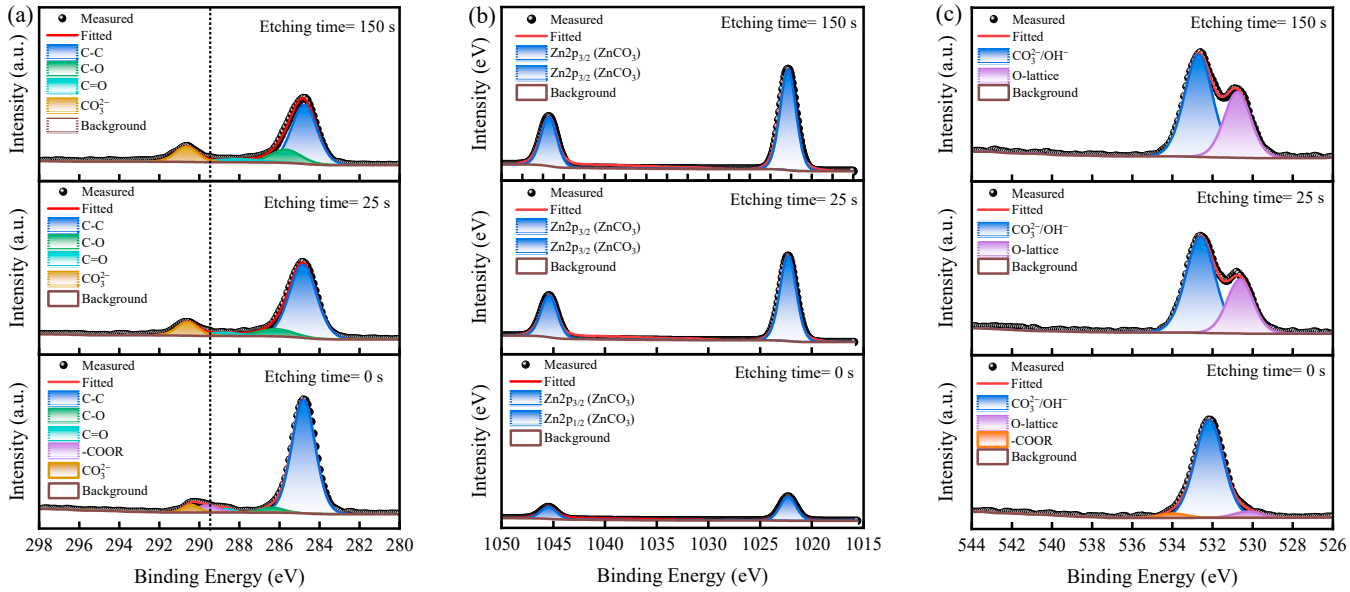

Figure 13. Depth profiling high-resolution XPS C 1s (**a**), Zn 2p (**b**) and O 1s (**c**) spectra of the smithsonite sample after conditioning with the sodium salt of 2-DMPT at pH 11.5.

Figure 13 presents the C 1s, Zn 2p, and O 1s XPS high-resolution spectra for the treated smithsonite sample at different etching times. In Figure 13a, the C 1s spectra of the bare smithsonite surface (etching time = 0 s) were fitted into five peaks for five different carbons: carbon in C–(C, H) bonds (284.80 eV), carbon in C–O bonds (286.37 eV), carbonyl carbon C=O (288.62 eV), carboxyl acid carbon (289.61 eV), and carbonate carbon CO_3^{2-} (290.40 eV) [48,49]. Compared to the C1s spectrum of the bare dolomite surface, the signal strength of carboxyl acid carbon on the bare smithsonite surface was notably weaker. Hence, it is speculated that the interaction between the saponified 2-DMPT and smithsonite surfaces in an alkaline medium of pH = 11.5 was relatively less pronounced than that with dolomite. As shown in Figure 13b, the Zn $2p_{3/2}$ and Zn $2p_{1/2}$ peaks of the bare smithsonite surface were located at the banding energy of 1022.30 and 1045.45 eV, respectively, indicating the oxidation state of the zinc species on the surface of smithsonite was +2.

Increasing etching time had little effect on the binding energy, but the Zn $2p_{3/2}$ photoelectron peak's signal was noticeably enhanced. Furthermore, in Figure 13c, the O 1s region demonstrates an extremely weak peak with BE of 533.94 eV associated with the oxygen atoms in carboxylic groups [50], which cannot be observed after a 25-s sputtering treatment. These results suggest that the chemical environment of zinc on the smithsonite surface remained relatively unchanged, but the amount of active sites (Zn^{2+}) was significantly reduced after treatment with saponified 2-DMPT at pH 11.5. Considering the weak signal of carboxyl acid carbon, which is related to the absorption of the collector, it is presumed that a considerable amount of hydroxide ion (OH^-) deactivated smithsonite surfaces by occupying the active Zn sites, leading to reduced flotation recovery and facilitating the reverse flotation separation of dolomite from smithsonite.

4. Conclusions

In this study, 2-(4,4-dimethylpentan-2-yl)-5,7,7-trimethyloctanoic acid was introduced as a potential collector for the reverse flotation of dolomite from smithsonite. The microflotation test results indicated that saponified 2-DMPT exhibited a stronger collecting ability and higher selectivity to dolomite compared to smithsonite under highly alkaline conditions, enabling efficient removal of dolomite from smithsonite through reverse flotation. At a collector concentration of 2.5×10^{-4} mol·L^{-1} and a pulp pH of 11.5, the floatability of dolomite reached 62%, whereas only 6% of smithsonite entered the flotation foam products. Zeta potential measurement and ATR-FTIR analysis provided insights into the adsorption behavior of saponified 2-DMPT. Increasing pH strongly hindered the adsorption of the collector onto the surface of smithsonite, while it had limited influence on dolomite. XPS analysis further confirmed the formation of hydrophobic complexes Ca^{2+}–COO–, resulting from the chemical reaction between carboxylic groups in the collector 2-DMPT and active Ca^{2+} sites on the dolomite surface. However, on the smithsonite surface, the signal of carboxyl acid carbon was weak, and the chemical environment of active Zn sites remained largely unchanged. In conclusion, 2-DMPT shows promising potential for the pre-removal of dolomite from smithsonite through reverse flotation, which can reduce acid consumption and facilitate the direct acid-leaching process of carbonate-rich zinc oxide ores. The findings of this study contribute to the economic and efficient exploitation of such zinc oxide ores using the beneficiation-hydrometallurgy coordination process.

Author Contributions: Investigation, data curation, formal analysis, visualization, writing—original draft, X.Z.; conceptualization, methodology, supervision, writing–review and editing, Y.Z.; project administration, resources, funding acquisition, Z.Z.; investigation, methodology, P.W. All authors have read and agreed to the published version of the manuscript.

Funding: This research was funded by the China Postdoctoral Science Foundation (2022M721432), and the Key Program for Science and Technology Innovation Foundation of BGRIMM Technology Group (Grant No. 02-2206).

Data Availability Statement: The data presented in this study are available upon request from the corresponding author.

Acknowledgments: The authors would like to thank Yueru Wu and Ruirong Zhang for the XPS and ATR-FTIR measurements.

Conflicts of Interest: The authors declare no conflict of interest.

References

1. U.S. Geological Survey. *Mineral Commodity Summaries 2023*; U.S. Geological Survey: Reston, VA, USA, 2023; 210p. [CrossRef]
2. Feng, D.; Bai, L.; Xie, H.; Tong, X. Study on Separation of Low-Grade Zinc Oxide Ore with Sulfurizationamination Flotation. *Physicochem. Probl. Miner. Process.* **2019**, *55*, 1082–1090.
3. Araújo, A.C.A.; Lima, R.M.F. Influence of Cations Ca^{2+}, Mg^{2+} and Zn^{2+} on the Flotation and Surface Charge of Smithsonite and Dolomite with Sodium Oleate and Sodium Silicate. *Int. J. Miner. Process.* **2017**, *167*, 35–41. [CrossRef]
4. Ejtemaei, M.; Irannajad, M.; Gharabaghi, M. Influence of Important Factors on Flotation of Zinc Oxide Mineral Using Cationic, Anionic and Mixed (Cationic/Anionic) Collectors. *Miner. Eng.* **2011**, *24*, 1402–1408. [CrossRef]

5. Irannajad, M.; Ejtemaei, M.; Gharabaghi, M. The Effect of Reagents on Selective Flotation of Smithsonite-Calcite-Quartz. *Miner. Eng.* **2009**, *22*, 766–771. [CrossRef]
6. Wang, L.; Hu, G.; Sun, W.; Khoso, S.A.; Liu, R.; Zhang, X. Selective Flotation of Smithsonite from Dolomite by Using Novel Mixed Collector System. *Trans. Nonferrous Met. Soc. China* **2019**, *29*, 1082–1089. [CrossRef]
7. Luo, B.; Liu, J.; Liu, Q.; Song, C.; Yu, L.; Li, S.; Lai, H. A Mechanism for the Adsorption of 2-(Hexadecanoylamino)Acetic Acid by Smithsonite: Surface Spectroscopy and Microflotation Experiments. *Minerals* **2019**, *9*, 15. [CrossRef]
8. Dhar, P.; Thornhill, M.; Kota, H.R. An Overview of Calcite Recovery by Flotation. *Mater. Circ. Econ.* **2020**, *2*, 9. [CrossRef]
9. Luo, Y.; Zhang, G.; Li, C.; Mai, Q.; Liu, H.; Zhou, H.; Shi, Q. Flotation Separation of Smithsonite from Calcite Using a New Depressant Fenugreek Gum. *Colloids Surf. A Physicochem. Eng. Asp.* **2019**, *582*, 123794. [CrossRef]
10. Zhou, H.; Yang, Z.; Zhang, Y.; Xie, F.; Luo, X. Flotation Separation of Smithsonite from Calcite by Using Flaxseed Gum as Depressant. *Miner. Eng.* **2021**, *167*, 106904. [CrossRef]
11. Yang, D.; Li, B.; Feng, D.; Xie, X.; Mo, F.; Tong, X.; Song, Q. Flotation Separation of Smithsonite from Calcite with Guar Gum as Depressant. *Colloids Surf. A Physicochem. Eng. Asp.* **2022**, *650*, 129562. [CrossRef]
12. Sun, H.; Niu, F.; Zhang, J. Investigation on the Flotation Separation of Smithsonite from Calcite Using Calcium Lignosulphonate as Depressant. *Colloids Surf. A Physicochem. Eng. Asp.* **2021**, *630*, 127571. [CrossRef]
13. Liu, C.; Wang, X.; Yang, S.; Ren, Z.; Li, C.; Hu, Z. Utilization of Polyepoxysuccinic Acid as a Green Depressant for the Flotation Separation of Smithsonite from Calcite. *Miner. Eng.* **2021**, *168*, 106933. [CrossRef]
14. Zeng, Y.; Yao, X.; Liu, G.; He, G.; Yu, X.; He, G.; Huang, Z.; Zhang, R.; Cheng, C. Flotation Behavior and Mechanism of Phenylpropenyl Hydroxamic Acid for the Separation of Smithsonite and Calcite. *J. Mol. Liq.* **2021**, *339*, 116893. [CrossRef]
15. Chen, Y.; Guo, X.; Chen, Y. Using Phytic Acid as a Depressant for the Selective Flotation Separation of Smithsonite from Calcite. *Sep. Purif. Technol.* **2022**, *302*, 122104. [CrossRef]
16. Liu, C.; Zhang, W.; Song, S.; Li, H.; Liu, Y. Flotation Separation of Smithsonite from Calcite Using 2-Phosphonobutane-1,2,4-Tricarboxylic Acid as a Depressant. *Powder Technol.* **2019**, *352*, 11–15. [CrossRef]
17. Wang, L.; Shen, L.; Sun, W.; Zhang, X.; Zhang, Y.; Wang, Y. Selective Flotation Separation of Smithsonite from Dolomite by Using Sodium Hexametaphosphate as a Depressant. *Colloids Surf. A Physicochem. Eng. Asp.* **2022**, *651*, 129621. [CrossRef]
18. Wang, L.; Lyu, W.; Zhou, W.; Zhang, H. The Role of Sodium Phytate in the Flotation Separation of Smithsonite from Calcite. *Miner. Eng.* **2022**, *187*, 107775. [CrossRef]
19. Feng, Q.; Wen, S.; Bai, X.; Chang, W.; Cui, C.; Zhao, W. Surface Modification of Smithsonite with Ammonia to Enhance the Formation of Sulfidization Products and Its Response to Flotation. *Miner. Eng.* **2019**, *137*, 1–9. [CrossRef]
20. Feng, Q.; Zhao, W.; Wen, S. Ammonia Modification for Enhancing Adsorption of Sulfide Species onto Malachite Surfaces and Implications for Flotation. *J. Alloys Compd.* **2018**, *744*, 301–309. [CrossRef]
21. Wang, M.; Zhang, G.; Chen, Y.; Zhao, L. Effect of Surface Oxidization on Quartz Slime Coating in the Sulfidization-Amine Flotation of Smithsonite. *Miner. Eng.* **2022**, *188*, 107847. [CrossRef]
22. Wei, Q.; Dong, L.; Qin, W.; Jiao, F.; Qi, Z.; Feng, C.; Sun, D.; Wang, L.; Xiao, S. Efficient Flotation Recovery of Lead and Zinc from Refractory Lead-Zinc Ores under Low Alkaline Conditions. *Geochemistry* **2021**, *81*, 125769. [CrossRef]
23. Wu, D.; Ma, W.; Wen, S.; Deng, J.; Bai, S. Enhancing the Sulfidation of Smithsonite by Superficial Dissolution with a Novel Complexing Agent. *Miner. Eng.* **2017**, *114*, 1–7. [CrossRef]
24. Ejtemaei, M.; Gharabaghi, M.; Irannajad, M. A Review of Zinc Oxide Mineral Beneficiation Using Flotation Method. *Adv. Colloid Interface Sci.* **2014**, *206*, 68–78. [CrossRef]
25. Ma, Z.; Wang, L.; Ni, X.; Liao, Y.; Liang, Z. Zinc Recovery from Wulagen Sulfide Flotation Plant Tail by Applying Ether Amine Organic Collectors. *Molecules* **2021**, *26*, 5365. [CrossRef] [PubMed]
26. Zhou, Q. Selective Flotation between Smithsonite and Calcite. Ph.D. Thesis, Central South University, Changsha, China, 2010.
27. Zhang, Y. Recovery Valuable Metals from Processing Gangue Minerals. Ph.D. Thesis, Autonomous University of San Luis Potosí, San Luis Potosí, Mexico, 2022.
28. Dehaine, Q.; Filippov, L.O.; Filippova, I.V.; Tijsseling, L.T.; Glass, H.J. Novel Approach for Processing Complex Carbonate-Rich Copper-Cobalt Mixed Ores via Reverse Flotation. *Miner. Eng.* **2021**, *161*, 106710. [CrossRef]
29. Zhang, Q.; Liu, R.; Cao, X.; Sun, W.; Yang, Y. Relationship between Structure and Property of Collecting Agent for Fatty Acids Scheelite. *Nonferrous Met. Sci. Eng.* **2013**, *4*, 85–90.
30. Sheng, Q.; Yin, W.; Yang, B.; Sun, H.; Yao, J. Efficiently Separating Malachite from Talc Using New Collector Famciclovir via Reverse Flotation. *Miner. Eng.* **2021**, *174*, 107243. [CrossRef]
31. Liu, G.; Kazarian, S.G. Recent Advances and Applications to Cultural Heritage Using ATR-FTIR Spectroscopy and ATR-FTIR Spectroscopic Imaging. *Analyst* **2022**, *147*, 1777–1797. [CrossRef]
32. Fuerstenau, D.W.; Pradip. Zeta Potentials in the Flotation of Oxide and Silicate Minerals. *Adv. Colloid Interface Sci.* **2005**, *114–115*, 9–26. [CrossRef]
33. Chen, X.; Liu, W.; Wang, L.; Liu, W.; Sun, W.; Zhang, N. A novel depressant N, N-bis (phosphonomethyl) glycine for magnesite-dolomite separation and its mechanism. *Miner. Eng.* **2023**, *202*, 108281. [CrossRef]
34. Zhang, J.; Xiao, Z.; Zhang, H. Selective Flotation Behavior of Dolomite from Fluorapatite Using Hydroxy Ethylene Diphosphonic Acid as High-Efficiency Depressant. *Minerals* **2022**, *12*, 1633. [CrossRef]

35. Shi, Q.; Feng, Q.; Zhang, G.; Deng, H. Electrokinetic properties of smithsonite and its floatability with anionic collector. *Colloids Surf. A Physicochem. Eng. Asp.* **2012**, *410*, 178–183. [CrossRef]
36. Zou, H.; Cao, Q.; Liu, D.; Yu, X.; Lai, H. Surface Features of Fluorapatite and Dolomite in the Reverse Flotation Process Using Sulfuric Acid as a Depressor. *Minerals* **2019**, *9*, 33. [CrossRef]
37. Yu, X.; Zhang, R.; Zeng, Y.; Cheng, C.; Huang, Z.; Wang, J.; He, G.; Wang, H. The Effect and Mechanism of Cinnamic Hydroxamic Acid as a Collector in Flotation Separation of Malachite and Calcite. *Miner. Eng.* **2021**, *164*, 106847. [CrossRef]
38. Cui, Y.; Jiao, F.; Wei, Q.; Wang, X.; Dong, L. Flotation Separation of Fluorite from Calcite Using Sulfonated Lignite as Depressant. *Sep. Purif. Technol.* **2020**, *242*, 116698. [CrossRef]
39. Liu, M.; Li, H.; Jiang, T.; Liu, Q. Flotation of Coarse and Fine Pyrochlore Using Octyl Hydroxamic Acid and Sodium Oleate. *Miner. Eng.* **2019**, *132*, 191–201. [CrossRef]
40. Ebajo, V.D.; Santos, C.R.L.; Alea, G.V.; Lin, Y.A.; Chen, C.H. Regenerable Acidity of Graphene Oxide in Promoting Multicomponent Organic Synthesis. *Sci. Rep.* **2019**, *9*, 15579. [CrossRef]
41. Dolgov, A.; Lopaev, D.; Lee, C.J.; Zoethout, E.; Medvedev, V.; Yakushev, O.; Bijkerk, F. Characterization of Carbon Contamination under Ion and Hot Atom Bombardment in a Tin-Plasma Extreme Ultraviolet Light Source. *Appl. Surf. Sci.* **2015**, *353*, 708–713. [CrossRef]
42. Yang, K.; Zhang, J.; Ma, X.; Ma, Y.; Kan, C.; Ma, H.; Li, Y.; Yuan, Y.; Liu, C. β-Tricalcium Phosphate/Poly(Glycerol Sebacate) Scaffolds with Robust Mechanical Property for Bone Tissue Engineering. *Mater. Sci. Eng. C* **2015**, *56*, 37–47. [CrossRef]
43. Xing, X.; Wang, B.; Liu, H.; Luo, S.; Wang, S.; Wei, J.; Xu, W.; Yu, Q. The Mechanism of Silane-Grafted Sodium Polyacrylate on the Toughening of Slag-Based Geopolymer: An Insight from Macroscopic–Microscopic Mechanical Properties. *J. Mater. Sci.* **2023**, *58*, 8757–8778. [CrossRef]
44. Yang, B.; Wang, D.; Cao, S.; Yin, W.; Xue, J.; Zhu, Z.; Fu, Y.; Yao, J. Selective Adsorption of a High-Performance Depressant onto Dolomite Causing Effective Flotation Separation of Magnesite from Dolomite. *J. Colloid Interface Sci.* **2020**, *578*, 290–303. [CrossRef]
45. Wang, Y.; Li, L.; Dai, P.; Yan, L.; Cao, L.; Gu, X.; Zhao, X. Missing-Node Directed Synthesis of Hierarchical Pores on a Zirconium Metal-Organic Framework with Tunable Porosity and Enhanced Surface Acidity: Via a Microdroplet Flow Reaction. *J. Mater. Chem. A* **2017**, *5*, 22372–22379. [CrossRef]
46. Li, J.P.H.; Zhou, X.; Pang, Y.; Zhu, L.; Vovk, E.I.; Cong, L.; Van Bavel, A.P.; Li, S.; Yang, Y. Understanding of Binding Energy Calibration in XPS of Lanthanum Oxide by: In Situ Treatment. *Phys. Chem. Chem. Phys.* **2019**, *21*, 22351–22358. [CrossRef]
47. Pang, Y.; Zhou, X.; Vovk, E.I.; Guan, C.; Li, S.; van Bavel, A.P.; Yang, Y. Understanding Lanthanum Oxide Surface Structure by DFT Simulation of Oxygen 1s Calibrated Binding Energy in XPS after in Situ Treatment. *Appl. Surf. Sci.* **2021**, *548*, 149214. [CrossRef]
48. Chen, X.; Wang, X.; Fang, D. A Review on C1s XPS-Spectra for Some Kinds of Carbon Materials. *Fuller. Nanotub. Carbon Nanostruct.* **2020**, *28*, 1048–1058. [CrossRef]
49. Li, C.; Bai, S.; Ding, Z.; Yu, P.; Wen, S. Visual MINTEQ Model, ToF–SIMS, and XPS Study of Smithsonite Surface Sulfidation Behavior: Zinc Sulfide Precipitation Adsorption. *J. Taiwan Inst. Chem. Eng.* **2019**, *96*, 53–62. [CrossRef]
50. Araújo, M.P.; Soares, O.S.G.P.; Fernandes, A.J.S.; Pereira, M.F.R.; Freire, C. Tuning the Surface Chemistry of Graphene Flakes: New Strategies for Selective Oxidation. *RSC Adv.* **2017**, *7*, 14290–14301. [CrossRef]